

# UC Irvine

## UC Irvine Previously Published Works

### Title

Assessing multi-site  $\delta^{18}\text{O}$ -climate calibrations of the coralline alga *Clathromorphum* across the high-latitude Northern Hemisphere

### Permalink

<https://escholarship.org/uc/item/4nk1c2kx>

### Authors

Ng, Jessica Y  
Williams, Branwen  
Thompson, Diane M  
[et al.](#)

### Publication Date

2016-12-01

### DOI

10.1016/j.gca.2016.08.023

Peer reviewed



# Assessing multi-site $\delta^{18}\text{O}$ -climate calibrations of the coralline alga *Clathromorphum* across the high-latitude Northern Hemisphere

Jessica Y. Ng<sup>a</sup>, Branwen Williams<sup>b,\*</sup>, Diane M. Thompson<sup>c</sup>, Chloe Mayne<sup>d</sup>,  
Jochen Halfar<sup>e</sup>, Evan Edinger<sup>f</sup>, Kathleen Johnson<sup>g</sup>

<sup>a</sup> Scripps College, 1030 Columbia Avenue, Claremont, CA 91711, USA

<sup>b</sup> W.M. Keck Science Department, Claremont McKenna College, Pitzer College, Scripps College, 925 N. Mills Avenue, Claremont, CA 91711, USA

<sup>c</sup> Climate & Global Dynamics, National Center for Atmospheric Research, PO Box 3000, Boulder, CO 80307, USA

<sup>d</sup> Pitzer College, 1030 Columbia Avenue, Claremont, CA 91711, USA

<sup>e</sup> University of Toronto Mississauga, 3359 Mississauga Rd, Mississauga, ON L5L 1C6, Canada

<sup>f</sup> Department of Geography, Memorial University of Newfoundland, St. John's, NL A1B 3X9, Canada

<sup>g</sup> Department of Earth System Science, University of California Irvine, 3200 Croul Hall, Irvine, CA 92697, USA

Received 12 April 2016; accepted in revised form 18 August 2016; available online 25 August 2016

## Abstract

An increased number of climate proxy records and more refined interpretation of proxy data are crucial to improve projections of future climate at high latitudes, where internal feedbacks amplify warming and established high-resolution climate archives are especially sparse. Encrusting coralline algae are being developed as a mid- to high-latitude marine climate archive. These long-lived algae form a solid high-Mg calcite skeleton with annual growth bands similar to those of trees and tropical corals. The oxygen isotope ratio of the algal skeleton ( $\delta^{18}\text{O}_{\text{alg}}$ ) records local environmental and climatic factors, notably sea surface temperature and seawater  $\delta^{18}\text{O}$ .

Here we assess the  $\delta^{18}\text{O}_{\text{alg}}$ -climate relationship in diverse environments across the algal habitat range utilizing two species of coralline algae from the genus *Clathromorphum*. *Clathromorphum* is widely distributed from the cold-temperate North Atlantic and Pacific to the Arctic Ocean and has recently yielded numerous climate reconstructions of up to 650 years in length. In this study, we calibrate  $\delta^{18}\text{O}_{\text{alg}}$  of four specimens to gridded temperature and salinity data, the latter a proxy for seawater  $\delta^{18}\text{O}$ . These specimens were collected from a variety of algal growth environments across the high-latitude Northern Hemisphere: two specimens from the Aleutian Archipelago, one from the Canadian Arctic, and one from the Gulf of Maine. Low winter temperatures and insolation restrict the months when algae record local climate in the  $\delta^{18}\text{O}$  of their skeletons; we therefore determine these response seasons by correlating monthly temperature and salinity anomalies with annual  $\delta^{18}\text{O}_{\text{alg}}$  anomalies at each site. We then average gridded data over months that correlate significantly (95% confidence interval) for regression with  $\delta^{18}\text{O}_{\text{alg}}$ . While the timing and nature of the climate signal vary across sites, we find significant relationships between  $\delta^{18}\text{O}_{\text{alg}}$  and either temperature or salinity averaged over the response season at three sites. Variation in local climatology among the four sites provides a physical explanation for calibration differences, compounded by uncertainties stemming from the proxy chronology, biological variability, temporal coverage, and sparse historical climate data. This work takes an essential step toward reconstructing high-latitude marine climate patterns with coralline algal  $\delta^{18}\text{O}$  and developing algae proxy system models.

© 2016 Elsevier Ltd. All rights reserved.

**Keywords:** Coralline algae; Sea surface temperature; Salinity; Paleoclimatology

\* Corresponding author.

E-mail address: [bwilliams@kecksci.claremont.edu](mailto:bwilliams@kecksci.claremont.edu) (B. Williams).

## 1. INTRODUCTION

Predicting the magnitude, nature, and pattern of continued anthropogenic climate change requires knowledge of natural climate variability on global to local scales. Reconstructions of past climate based on paleoclimate “proxy” records supplement instrumental records to inform our scientific understanding of climate mechanisms, natural baselines, rates of change, and possible extremes. However, sparse instrumental measurements prior to the late 20th century and across many regions limit the utility of these data sets to studying recent climate variability (e.g. Brohan et al., 2006). Climate proxies, i.e. climate-dependent chemical and physical properties of datable biological or geological archives, extend the spatial and temporal coverage of historical observations (PAGES 2k Consortium, 2013). These proxies help constrain climate sensitivity and thus the range of past and future climates simulated by climate models (e.g. Hegerl et al., 2006). Over a broad spatial range, they can also lend insight into large-scale climate patterns (e.g. corals and ENSO in Evans et al., 2000; Thompson et al., 2011).

Improvements in our ability to extract climate signals from proxy data are critical in Arctic and sub-Arctic regions, where highly productive ecosystems support enormous fisheries (Stabeno et al., 1999) and where temperature increases are the greatest as internal feedbacks amplify anthropogenic warming (Kirtman et al., 2013). The mechanism behind this polar amplification is well-documented: warming increases sea-ice melt, exposing greater area of low-albedo ocean surface for a longer portion of the year; the decrease in albedo then increases heat absorption, amplifying the initial warming (e.g. Curry et al., 1995). However, large uncertainties remain in the rate of sea-ice loss, and thus in the contribution of this ice-albedo feedback to warming (Meehl et al., 2012, 2013). Representation of these processes is therefore a source of uncertainty in climate model projections. An improved understanding of past high-latitude ocean variability is key to projecting future high-latitude climate, its impacts, and its interaction with the global climate system.

Encrusting coralline algae are being increasingly developed as a high-resolution archive of northern marine climate (Adey et al., 2013). Coralline algae add unique information to the network of available marine archives, reaching higher latitudes than tropical corals and expanding the spatial distribution beyond that of bivalves, which are commonly used for multicentury reconstructions in the temperate and subarctic North Atlantic (e.g. Surge and Barrett, 2012; Wanamaker et al., 2012; Butler et al., 2013). While the physiology and ecology of these algae have been described in depth (e.g. Adey, 1965; Lebednik, 1976; summarized in Adey et al., 2013), they have only recently been applied to marine paleoclimate reconstructions (e.g. Halfar et al., 2007; Kamenos et al., 2008; Hetzinger et al., 2009; Hetzinger et al., 2012; Kamenos et al., 2012; Williams et al., 2014). An improved understanding of the algae–climate relationship is therefore necessary for these archives to be used alongside other high-resolution climate archives (e.g. tree rings, corals) in analysis of large-scale cli-

mate variability and dynamics. Empirical calibrations of the algae–climate relationship that we present here provide the foundation for mechanistic models and coralline algae proxy system models (PSMs). The PSM method mathematically portrays the physical, chemical, and biological processes by which climate is incorporated into proxy records (Evans et al., 2013; Dee et al., 2016). PSMs thereby provide an alternative approach to paired measurements (e.g.  $\delta^{18}\text{O}$  with Mg/Ca in Kamenos et al., 2012) for assessing the contribution of climatic factors (such as seawater temperature and salinity) to coralline algal  $\delta^{18}\text{O}$ . In addition, PSMs may be used to test uncertainties in global climate models, historical observations, and the coralline algal proxy records themselves (e.g. Schmidt, 1999; Thompson et al., 2011).

The coralline alga *Clathromorphum* covers a wide latitudinal and longitudinal range (Fig. 1) and can live for hundreds of years (Adey et al., 2013; Halfar et al., 2013); thus it holds potential to fill in substantial geographic and temporal gaps in the proxy data available in temperate to Arctic regions. The alga calcifies a high-Mg calcite skeleton with distinct annual growth layers, which can be accurately dated and sampled with subannual resolution. The resolution of resulting records depends largely on growth rates, which range from greater than 400  $\mu\text{m}/\text{year}$  in specimens from the Aleutian Archipelago to less than 100  $\mu\text{m}/\text{year}$  in Arctic specimens (Adey, 1965; Adey et al., 2013).

The stable oxygen isotope ratio  $\delta^{18}\text{O}$  of the algal skeleton ( $\delta^{18}\text{O}_{\text{alg}}$ ) depends on sea surface temperature (SST) and seawater  $\delta^{18}\text{O}$  ( $\delta^{18}\text{O}_{\text{sw}}$ ) (Moberly, 1968), which varies with sea surface salinity (SSS, see 3.2 Salinity as a proxy for seawater  $\delta^{18}\text{O}$ ). While systematic calibration of  $\delta^{18}\text{O}_{\text{alg}}$  records to the ambient environment has been limited by a lack of in situ SST and SSS observations and high-resolution  $\delta^{18}\text{O}_{\text{alg}}$  records, major steps have been taken in the past decade toward applying  $\delta^{18}\text{O}_{\text{alg}}$  to understand marine paleoclimate. Halfar et al. (2007) found that the first 117-year record of  $\delta^{18}\text{O}_{\text{alg}}$  from Attu Island, Alaska, significantly correlated with a single June–November coarse-resolution gridded and interpolated SST data set. They used the  $\delta^{18}\text{O}_{\text{alg}}$  record to reconstruct variability in the El

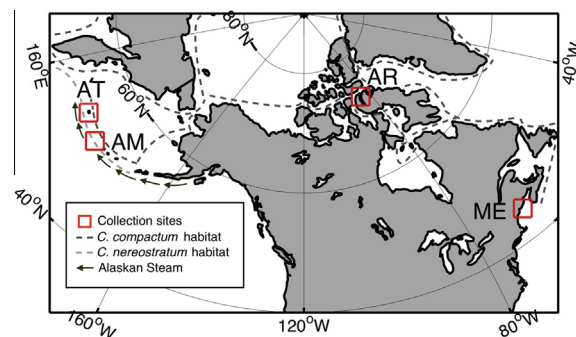


Fig. 1. Coralline algae specimens were collected from Amchitka (AM) and Attu (AT) Islands along the Aleutian Archipelago, Arctic Bay (AR) in northern Canada, and the Gulf of Maine (ME). Habitat ranges (dashed lines) of the *Clathromorphum* specimens used here were taken from Adey et al. (2013). The Alaskan Stream (arrows) may influence environment of the Aleutian specimens.

Niño-Southern Oscillation and the Pacific Decadal Oscillation influencing the central Aleutian archipelago. In a second study, Halfar et al. (2008) found that a 30-year  $\delta^{18}\text{O}_{\text{alg}}$  record from the Gulf of Maine significantly correlated with May–December in situ instrumental SST data (Halfar et al., 2008). These early studies demonstrate the potential for  $\delta^{18}\text{O}_{\text{alg}}$  in coralline algae as a climate proxy to reconstruct past high-latitude climate variability.

We anticipate the application of  $\delta^{18}\text{O}_{\text{alg}}$  to both forward (i.e. PSMs) and inverse (i.e. climate reconstruction) models at diverse locations spanning the wide latitudinal and longitudinal range of coralline algae. However, the two studies described above used disparate methods, SST data sets, and locations to analyze the  $\delta^{18}\text{O}_{\text{alg}}$ –SST relationship, preventing a direct comparison between the resulting relationships and therefore limiting their application in larger scale climate reconstructions or PSMs. Furthermore, the calibration methods applied in Halfar et al. (2008) may not be feasible at all sites; for example, low growth rates in northernmost habitats prohibit subannual calibration, and long term in-situ observations are rare along the Aleutian Islands. In addition, no studies to date have investigated the influence  $\delta^{18}\text{O}_{\text{sw}}$  (or SSS) variability on  $\delta^{18}\text{O}_{\text{alg}}$ . Finally, the SST and SSS variability of each site determines the signal to noise ratio and thus may influence the proxy sensitivity to climate in each specimen (e.g. Correge, 2006; de Vernal et al., 2006). Thus, additional and systematic calibration studies are needed to quantitatively assess  $\delta^{18}\text{O}$  in this coralline algae genus across a wide range of habitats.

Here we constrain the  $\delta^{18}\text{O}_{\text{alg}}$ –SST and  $\delta^{18}\text{O}_{\text{alg}}$ –SSS relationships by calibrating  $\delta^{18}\text{O}_{\text{alg}}$  of four specimens from across the algal habitat range to gridded marine data sets (Fig. 1): two specimens from Amchitka and Attu Islands along the Aleutian Archipelago, one from Arctic Bay in northern Canada, and one from the Gulf of Maine. After describing local climatology using two different gridded SST data sets, we determine the response season when the algal record local climate by correlating annual  $\delta^{18}\text{O}_{\text{alg}}$  anomalies with monthly SST and SSS anomalies from gridded marine data sets. We then assess the  $\delta^{18}\text{O}_{\text{alg}}$ –SST and  $\delta^{18}\text{O}_{\text{alg}}$ –SSS relationships at each collection site by averaging the months when  $\delta^{18}\text{O}_{\text{alg}}$  displays a significant correlation with the gridded marine data sets at the 95% confidence interval and regressing the average SST and SSS of these months with  $\delta^{18}\text{O}_{\text{alg}}$ . Finally, we compare the coefficients and the strength of the regression among sites. This study aims to improve our understanding of the  $\delta^{18}\text{O}_{\text{alg}}$ –climate relationship, assess whether a unified calibration may be found across diverse environments, and provide a foundation for developing coralline algal PSMs.

## 2. CLIMATOLOGY

We characterized intra-annual and inter-annual variability in SST and SSS as potential drivers of  $\delta^{18}\text{O}_{\text{alg}}$  variability at each site. To assess intra-annual variability at each site, we took the average SST and SSS of each month over the time period of the algal records (Fig. 2, Table 1). We calculated the standard deviation of the monthly averages as a

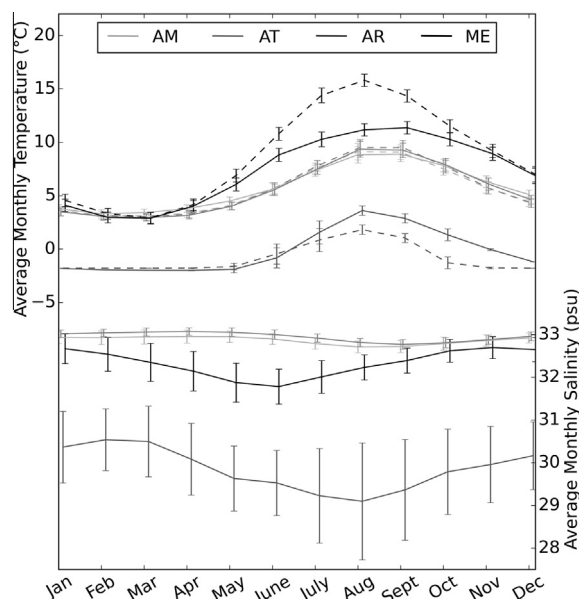


Fig. 2. Average monthly gridded SST (top, left axis) and SSS (bottom, right axis) at collection sites.  $\pm 1$  st. dev. in error bars indicates timing and magnitude of inter-annual variability. Dashed lines indicate NOAA ERSST; solid lines indicate SODA SST and SSS. Data points and error bars are slightly offset on the x-axis to avoid overlapping on the y-axis. Climatology was determined over the time span of the algae record at each site; i.e. 1968–2003 for Amchitka and Attu Islands, 1967–2008 for Arctic Bay, and 1977–2001 for Gulf of Maine.

measure of inter-annual variability. We used two gridded SST data sets, National Oceanic and Atmospheric Administration Extended Reconstructed SST version 4 (NOAA ERSST) and Simple Ocean Data Assimilation version 2.2.4 (SODA) SST, and one SSS data set, SODA SSS (see 3.1 Calibration with gridded marine data sets).

Intra-annual and inter-annual variability were similar at Amchitka and Attu Islands (determined over the period of the algal record, 1968–2003), which are both fed by the Alaskan Stream (Figs. 1 and 2) (Stabeno et al., 1999; Niebauer et al., 1999). Amchitka Island SST was lowest during March for NOAA ERSST (3.1 °C) and February for SODA SST (3.3 °C), and peaked during August–September for NOAA ERSST (9.1 °C) and September for SODA SST (8.9 °C). Inter-annual variability was greatest in August for NOAA ERSST (st. dev. =  $\pm 0.77$  °C) and September for SODA SST ( $\pm 0.87$  °C). SSS was highest in April–May (32.9 psu) and lowest in August (32.7 psu), while the greatest inter-annual variability occurred in March ( $\pm 0.17$  psu) with a secondary peak in October ( $\pm 0.15$  psu). At Attu Island, SST was lowest during March for both NOAA ERSST and SODA SST (3.0 and 2.9 °C, respectively) and peaked during August–September for NOAA ERSST (9.5 °C) and SODA SST (9.3 °C), with greatest inter-annual variability in August for NOAA ERSST ( $\pm 0.74$  °C) and November for SODA SST ( $\pm 0.72$  °C). SSS was highest in April (33.0 psu) and lowest in August (32.8 psu), with the greatest inter-annual variability of  $\pm 0.12$  psu during September–October and a secondary peak of  $\pm 0.11$  psu in June.

Table 1  
Description of the four specimens used in this study.

Specimen	Abbreviation	Latitude	Longitude	Years	Sampling resolution (samples/year)	SST response season	SSS response season
Amchitka	AM	51°25N	179°14E	1968–2003	1–12	Mar-May, Dec (SODA)	None
Attu	AT	52°47N	173°10E	1968–2003	3–10	July-Aug (NOAA); May-Aug (SODA)	None
Arctic Bay	AR	73°15N*	85°15W*	1967–2008	0–1	None	Jan-Feb, May–June, Aug-Oct
Maine	ME	44°08N	68°15W	1977–2001	4–8	None	Feb-June

\* Location is approximated for dredged Arctic Bay specimen.

Intra-annual and inter-annual SST variability at Arctic Bay (determined for the period 1967–2008) was restricted to late spring through winter because the subtidal seafloor is under ice during winter and spring (Fig. 2). A minimum SST of  $-1.8\text{ }^{\circ}\text{C}$  persisted December–April for NOAA ERSST, or  $-2.0\text{ }^{\circ}\text{C}$  during February–April for SODA SST, before SST rose toward an August maximum of  $1.8\text{ }^{\circ}\text{C}$  for NOAA ERSST and  $3.6\text{ }^{\circ}\text{C}$  for SODA SST. The greatest inter-annual variability occurred in July for NOAA ERSST ( $\pm 1.0\text{ }^{\circ}\text{C}$ ) and August for SODA SST ( $\pm 1.5\text{ }^{\circ}\text{C}$ ). Annual ice formation and melt resulted in the greatest SSS range here among the four sites. SSS rose to a February–March maximum of 30.5 psu as freshwater froze out, and then decreased to an August–September minimum of 29.1 psu from summer ice melt; inter-annual variability was greatest in August ( $\pm 1.14\text{ psu}$ ).

Intra-annual SST variability was the greatest at the Maine site (determined 1977–2001, Fig. 2), but the discrepancy between the two SST data sets was also largest at this

site. SST was lowest during March for both NOAA ERSST and SODA SST ( $2.9\text{ }^{\circ}\text{C}$ ); the highest SST occurred in August for NOAA ERSST ( $15.8\text{ }^{\circ}\text{C}$ ) and September for SODA SST ( $11.4\text{ }^{\circ}\text{C}$ ). Inter-annual SST variability was greatest in December for NOAA ERSST ( $\pm 0.72\text{ }^{\circ}\text{C}$ ) and September for SODA SST ( $\pm 1.5\text{ }^{\circ}\text{C}$ ). SSS peaked at 32.7 psu in November after a June minimum of 31.8 psu. The greatest inter-annual variability occurred April–May ( $\pm 0.46\text{ psu}$ ).

### 3. METHODS

#### 3.1. Encrusting coralline algae

*Clathromorphum* sp. specimens were collected from Amchitka Island ( $51^{\circ}25\text{N}$ ,  $179^{\circ}14\text{E}$ ) and Attu Island ( $52^{\circ}47\text{N}$ ,  $173^{\circ}10\text{E}$ ) in 2004, Arctic Bay in 2009 (dredged, appx.  $73^{\circ}15\text{N}$ ,  $85^{\circ}15\text{W}$ ), and Maine in 2002 ( $44^{\circ}08\text{N}$ ,  $68^{\circ}15\text{W}$ ) (Fig. 1, Table 1). The Aleutian specimens were *C. nereostrea-*

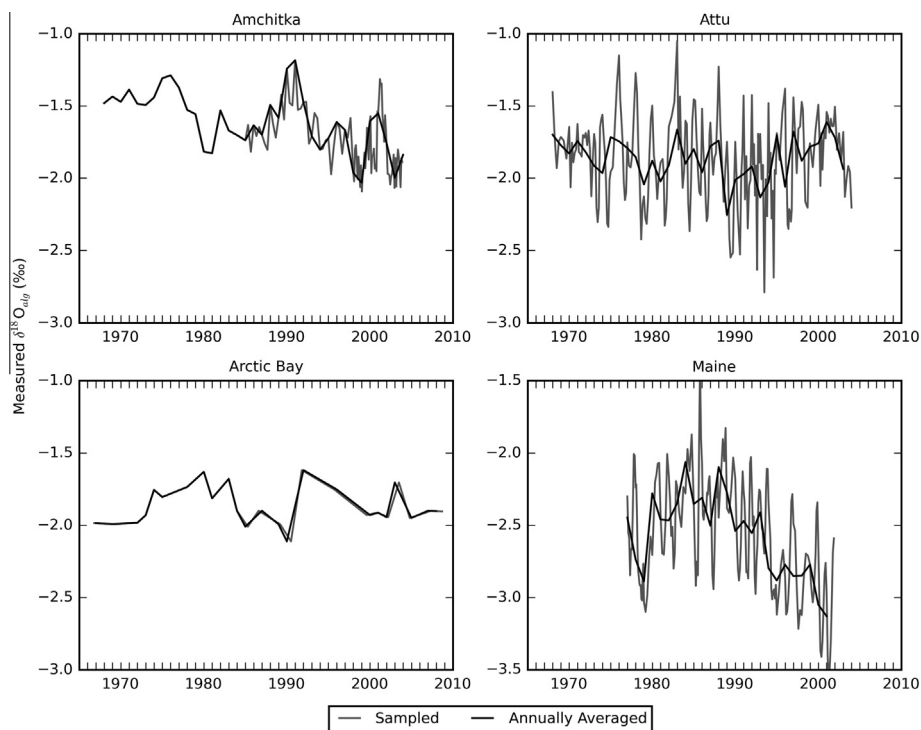


Fig. 3. Time series of sampled (gray) and annually averaged (black)  $\delta^{18}\text{O}_{\text{alg}}$  for each alga.

*tum* collected at 10 m depth (Halfar et al., 2011), and the Arctic and Maine specimens were *C. compactum* collected between 15 and 17 m and at 7 m, respectively (Halfar et al., 2008, 2013). We analyzed 36 years (1968–2003) in the Aleutian specimens, constrained by the collection year and Amchitka specimen age, and 25 years (1977–2001) in the Maine specimen, also constrained by collection year and age. The specimens were drilled using a high-precision, computer-driven micromill attached to an x, y, and z stage using digitized milling path positions as outlined in Williams et al. (2011) for the Amchitka specimen, Halfar et al. (2007) for the Attu specimen, and Halfar et al. (2008) for the Maine specimen (Fig. 3).

We show the Arctic Bay specimen  $\delta^{18}\text{O}_{\text{alg}}$  time series here for the first time (Fig. 3).  $\delta^{18}\text{O}_{\text{alg}}$  was measured from 50 to 70  $\mu\text{g}$  powdered calcite samples using a Kiel IV-carbonate device coupled with a ThermoFinnigan Delta V Plus isotope ratio mass spectrometer. Each run of 30 unknown samples included 16 standards (NBS-19, NBS-18 and OX, an in-house quality control standard), with a standard deviation of 0.06‰ for repeated NBS-19 measurements. Low growth rates limited the resolution of the Arctic Bay specimen, as the amount of material needed for a single measurement sometimes exceeded the amount the alga grew in a single year. Visually defined annual growth increments determined the chronology, yielding a resolution of approximately 1.35 years per sample (0.74 samples per year). The entire algal record extended to 1912; however, we limited our analysis to the period 1967–2008 due to large uncertainty in the chronology before 1960, several missing years of  $\delta^{18}\text{O}_{\text{alg}}$  between 1960 and 1967 caused by insufficient sample amounts, and the end of the SODA SST and SSS data sets at 2008.

### 3.2. Salinity as a proxy for seawater $\delta^{18}\text{O}$

We approximated seawater  $\delta^{18}\text{O}$  ( $\delta^{18}\text{O}_{\text{sw}}$ ) with SSS, for which data are far more abundant than for  $\delta^{18}\text{O}_{\text{sw}}$  (e.g. Epstein et al., 1951; LeGrande and Schmidt, 2006). The processes that lower SSS, such as precipitation and inflow of sea-ice melt, similarly lower  $\delta^{18}\text{O}_{\text{sw}}$  by introducing  $^{18}\text{O}$ -depleted fresh water. The processes that increase SSS, such as evaporation and freezing of sea ice, similarly increase  $\delta^{18}\text{O}_{\text{sw}}$  by removing  $^{18}\text{O}$ -depleted fresh water. Thus, both parameters reflect ice volume, cyclone activity, local currents, precipitation-evaporation budget, and source water and are strongly related throughout the global oceans, though the slope of this relationship varies regionally (e.g. LeGrande and Schmidt, 2006).

### 3.3. Gridded marine data sets

We compared  $\delta^{18}\text{O}_{\text{alg}}$  to SST from both NOAA ERSST (Huang et al., 2015) and SODA (SODA SST) (Carton and Giese, 2008), and to SSS from SODA (SODA SSS) (see descriptions below). We used grid boxes at the highest resolution for each data set ( $2^\circ \times 2^\circ$  for NOAA ERSST and  $0.5^\circ \times 0.5^\circ$  for SODA). NOAA ERSST grid boxes were centered at  $52^\circ\text{N}$ ,  $180^\circ\text{E}$  for Amchitka Island;  $52^\circ\text{N}$ ,  $172^\circ\text{E}$  for Attu Island;  $74^\circ\text{N}$ ,  $86^\circ\text{W}$  for Arctic Bay; and

$44^\circ\text{N}$ ,  $68^\circ\text{W}$  for Maine. SODA SST and SSS grid boxes were centered at  $51.25^\circ\text{N}$ ,  $179.25^\circ\text{E}$  for Amchitka Island;  $52.75^\circ\text{N}$ ,  $173.25^\circ\text{E}$  for Attu Island;  $73.25^\circ\text{N}$ ,  $85.25^\circ\text{W}$  for Arctic Bay; and  $44.25^\circ\text{N}$ ,  $68.25^\circ\text{W}$  for Maine. We selected the depth closest to the depth of sample collection for SODA SST and SSS at all sites (5 m for Attu and Amchitka Islands, 15 m for Arctic Bay, and 5 m for Maine); NOAA ERSST gives only surface temperatures. We evaluated both NOAA ERSST and SODA SST because the data set that best represents each site depends on the number and quality of observations for each grid box incorporated into globally gridded data sets and the methods by which observations were incorporated. We correlated these SST data sets with each other for each month to assess the agreement between these gridded data sets (see 4.1 Comparison of gridded marine data sets).

NOAA ERSST is a  $2^\circ \times 2^\circ$  global monthly SST data set with data from 1854 to the present using International Comprehensive Ocean–Atmosphere Data Set (ICOADS) as the primary data source. Version 4 includes more recent observations added to ICOADS release 2.5 and improved bias adjustments compared to previous versions (Huang et al., 2015; Liu et al., 2015).

SODA is a  $0.5^\circ \times 0.5^\circ$  global monthly marine climate reanalysis product that uses an ocean general circulation model with Parallel Ocean Program numerics, continuously corrected with observations. SST and SSS observations are sourced from the World Ocean Database (WOD), the U.S. National Oceanographic Data Center archive, in situ measurements, and SST determined using satellite remote sensing. Version 2.2.4 is a 2010 beta release product for 1871 to 2008, the first assimilation run over 100 years long as an extension from the original 1958–2001 version. Since we only used 1963 and later, we did not expect potential uncertainty in the early years of the beta run to interfere with our analysis (Carton and Giese, 2008).

### 3.4. DENDROCLIM2002

We used DENDROCLIM2002 to determine the response season when  $\delta^{18}\text{O}_{\text{alg}}$  records the climate signal (Fig. 4) (Biondi and Waikul, 2004). DENDROCLIM2002 is a software package developed to calibrate tree-ring chronologies with instrumental climate records (e.g. Cullen and Grierson, 2009; Huang et al., 2010; Liang et al., 2014). Tree rings are a similar proxy system to encrusting algae in that multiple climate signals are recorded seasonally in annual growth layers (e.g. Fritts, 1976). DENDROCLIM2002 computes Pearson's product moment correlation and response functions for each month using bootstrapped confidence intervals to assess statistical significance, which decreases the risk of underestimating error estimates (Biondi and Waikul, 2004).

### 3.5. Data analysis

We calculated anomalies by subtracting monthly means from gridded SST and SSS and subtracting the mean of the entire period from  $\delta^{18}\text{O}_{\text{alg}}$  to remove the potential impact of vital effects on the  $\delta^{18}\text{O}$  composition of the algae, assuming

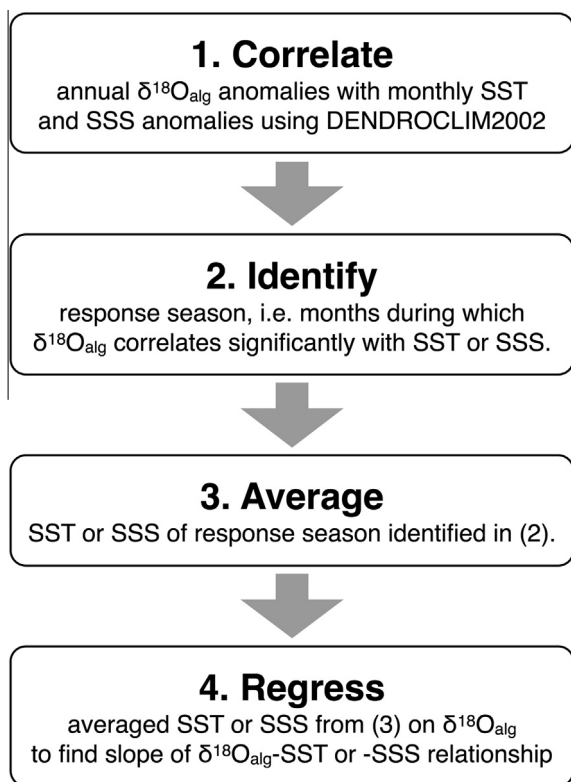


Fig. 4. Flowchart of data analysis methods used in this study.

that this impact is consistent over time (Lee and Carpenter, 2001; Halfar et al., 2007). Using DENDROCLIM2002, we correlated annual  $\delta^{18}\text{O}_{\text{alg}}$  anomalies with monthly SST and SSS anomalies from the gridded data sets to identify months with a significant correlation function at the 95% confidence level (Fig. 4). These months represented the response season, i.e. the periods when the algae were growing and recording local climate in the  $\delta^{18}\text{O}_{\text{alg}}$  of their skeletons. We found identical months of significant correlation between raw  $\delta^{18}\text{O}_{\text{alg}}$  and gridded data sets as with the anomalies, indicating that these months reflect when the algae record both intra- and inter-annual SST and SSS variability. We therefore averaged gridded SST and SSS anomalies for these significant months and regressed the averages with annually resolved  $\delta^{18}\text{O}_{\text{alg}}$  using an ordinary least squares regression (due to lack of error estimates for NOAA ERSST version 4 and SODA 2.2.4 for a reduced major axis least squares regression) to determine the  $\delta^{18}\text{O}_{\text{alg}}$ -climate relationship at each site (Fig. 4).

## 4. RESULTS

### 4.1. Comparison of gridded marine data sets

NOAA ERSST and SODA SST were significantly correlated ( $p < 0.05$ ) at Amchitka Island for all months ( $n = 36$ ), Attu Island for 10 months (February–November,  $n = 36$ ), and Maine for 6 months (January–April, October, and December,  $n = 25$ , Fig. S1). However, these temperature data sets were not significantly correlated over any months

at Arctic Bay ( $n = 42$ , Fig. S1). To determine whether the SST and SSS signals may have been coupled, we correlated monthly SST and SSS anomalies with each other at each site (Fig. S2). SST significantly varied with SSS at Amchitka Island during August–September for NOAA ERSST and September for SODA SST; at Attu Island during June–July for NOAA ERSST; at Arctic Bay during August–September for NOAA ERSST and during January and March–April for SODA SST; and at Maine during November for NOAA ERSST.

### 4.2. Monthly correlations to identify response season

Correlations of monthly gridded SST and SSS anomalies with  $\delta^{18}\text{O}_{\text{alg}}$  using DENDROCLIM2002 provided the response seasons when the algae recorded marine climate in their skeletal  $\delta^{18}\text{O}$  (Figs. 4 and 5). Amchitka  $\delta^{18}\text{O}_{\text{alg}}$  significantly correlated ( $p < 0.05$ ) with SODA SST during March ( $r = -0.40$ ,  $n = 36$  for all months), April ( $r = -0.32$ ), May ( $r = -0.36$ ), and December ( $r = -0.33$ ). NOAA ERSST and SODA SSS did not significantly correlate with  $\delta^{18}\text{O}_{\text{alg}}$  for any month. Attu  $\delta^{18}\text{O}_{\text{alg}}$  significantly correlated ( $p < 0.05$ ) with NOAA ERSST during July ( $r = -0.39$ ,  $n = 36$  for all months) and August ( $r = -0.33$ ), and with SODA SST during May ( $r = -0.43$ ), June ( $r = -0.53$ ), July ( $r = -0.41$ ), and August ( $r = -0.33$ ), while  $\delta^{18}\text{O}_{\text{alg}}$  did not significantly correlate with SSS during any month. Arctic Bay  $\delta^{18}\text{O}_{\text{alg}}$  did not significantly correlate with SST during any month, but did significantly correlate ( $p < 0.05$ ) with SSS during January ( $r = 0.27$ ,  $n = 42$  for all months), February ( $r = 0.35$ ), May ( $r = 0.35$ ), June ( $r = 0.33$ ), August ( $r = 0.31$ ), September ( $r = 0.41$ ) and October ( $r = 0.37$ ). Maine SST did not significantly correlate with  $\delta^{18}\text{O}_{\text{alg}}$ , but SSS significantly correlated with  $\delta^{18}\text{O}_{\text{alg}}$  during February ( $r = 0.39$ ,  $n = 25$  for all months), March ( $r = 0.35$ ), April ( $r = 0.31$ ), May ( $r = 0.35$ ), and June ( $r = 0.38$ ).

### 4.3. Regression over response season

To calibrate  $\delta^{18}\text{O}_{\text{alg}}$  to climate over the response season, we averaged SST anomalies for the Amchitka and Attu sites and SSS anomalies for the Arctic Bay and Maine sites over the months described above (Fig. 4). We then performed a least squares regression of annually resolved  $\delta^{18}\text{O}_{\text{alg}}$  with these averaged response season SST or SSS anomalies at each site (Figs. 4 and 6, S3).  $\delta^{18}\text{O}_{\text{alg}}$  was significantly related at the 95% confidence level to either SST or SSS at Amchitka Island, Attu Island, and Arctic Bay (Fig. 6, Table 2). Amchitka  $\delta^{18}\text{O}_{\text{alg}}$  was significantly related to SODA SST averaged over March–May and December (slope =  $-0.23\text{‰ }^{\circ}\text{C}^{-1}$ ,  $R^2 = 0.20$ ,  $p = 0.0063$ ,  $n = 36$ ). Attu  $\delta^{18}\text{O}_{\text{alg}}$  was significantly related to NOAA ERSST averaged over July–August and October–November (slope =  $-0.09\text{‰ }^{\circ}\text{C}^{-1}$ ,  $R^2 = 0.13$ ,  $p = 0.031$ ,  $n = 36$ ) and with SODA SST averaged over May–August (slope =  $-0.14\text{‰ }^{\circ}\text{C}^{-1}$ ,  $R^2 = 0.26$ ,  $p = 0.0017$ ,  $n = 36$ ). Arctic Bay  $\delta^{18}\text{O}_{\text{alg}}$  was significantly related to SSS averaged over January–February, May–June, and August–October (slope =  $0.072\text{‰ } \text{psu}^{-1}$ ,  $R^2 = 0.19$ ,  $p = 0.0041$ ,  $n = 42$ ).

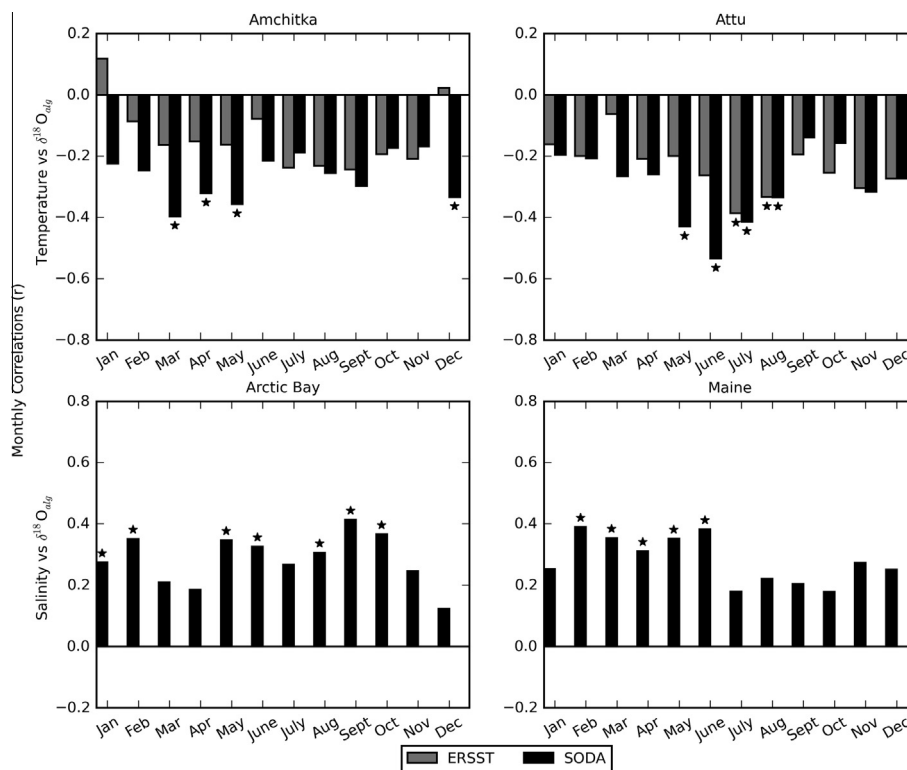


Fig. 5. Top row: monthly correlations ( $p < 0.05$ ) between NOAA ERSST and annually resolved  $\delta^{18}\text{O}_{\text{alg}}$  (gray) and between SODA SST and  $\delta^{18}\text{O}_{\text{alg}}$  (black), which imply months in which SST is recorded in  $\delta^{18}\text{O}_{\text{alg}}$  (Amchitka  $n = 36$ , Attu  $n = 36$ ). Bottom row: Monthly correlations between SSS and  $\delta^{18}\text{O}_{\text{alg}}$ , which imply months in which SSS is recorded in  $\delta^{18}\text{O}_{\text{alg}}$  (Arctic Bay  $n = 42$ , Maine  $n = 25$ ). Correlation analysis was performed on anomalies of all data sets, i.e. raw data minus means (monthly for SST and SSS, over the entire time period for  $\delta^{18}\text{O}_{\text{alg}}$ ). Asterisks (\*) indicate significant correlations at the 95% confidence level.

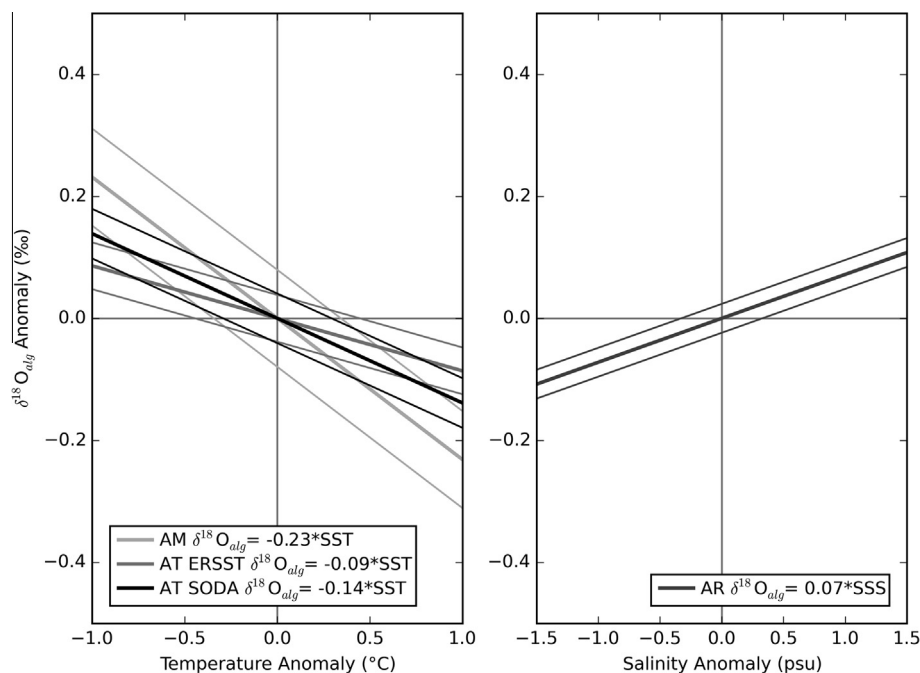


Fig. 6. Significant calibrations (i.e. least squares regressions at the 95% confidence level) of  $\delta^{18}\text{O}_{\text{alg}}$  with gridded SST (left) and SSS (right) averaged over the response seasons indicated in Fig. 5. Thick lines are slope  $\times$  using slope of the  $\delta^{18}\text{O}_{\text{alg}}$ -SST and  $\delta^{18}\text{O}_{\text{alg}}$ -SSS regression; equations given in legend. Thin lines are slope  $\times \pm 1$  st. err. of the regression. Regression analysis was performed on anomalies of all data sets, i.e. raw data minus means (monthly for SST and SSS, over the entire time period for  $\delta^{18}\text{O}_{\text{alg}}$ ).



Table 2

Statistics for the regression of  $\delta^{18}\text{O}_{\text{alg}}$  anomalies on gridded SST (for Amchitka and Attu) and SSS (for Arctic Bay and Maine) anomalies averaged over the months indicated in Fig. 5. The Durbin–Watson statistic (D–W) indicates minor serial correlation of Amchitka, Arctic Bay, and Maine regression residuals.

Specimen	Regressed with	<i>n</i>	Slope	<i>R</i> <sup>2</sup>	<i>p</i>	St. err.	D–W
AM	SODA SST	36	−0.23	0.2	0.0063	0.08	1.09
AT	NOAA ERSST	36	−0.09	0.13	0.031	0.038	1.53
	SODA SST	36	−0.14	0.26	0.0017	0.041	1.68
AR	SODA SSS	42	0.072	0.19	0.0041	0.024	0.7
ME	SODA SSS	25	0.27	0.15	0.057	0.14	0.96

Maine  $\delta^{18}\text{O}_{\text{alg}}$  was related to SSS averaged over February–June (slope =  $0.27\text{‰}\text{psu}^{-1}$ ,  $R^2 = 0.15$ ,  $p = 0.057$ ,  $n = 25$ ). Using a Durbin–Watson test, we observed minor positive serial correlation of the regression residuals at Amchitka Island, Arctic Bay, and Maine (Table 2).

The direction of the climate– $\delta^{18}\text{O}_{\text{alg}}$  relationship was consistent for SST regressions with *C. nereostratum* and for SSS regressions with *C. compactum* (Fig. 6, Table 2). Significant negative slopes for Amchitka Island  $\delta^{18}\text{O}_{\text{alg}}$  and Attu Island  $\delta^{18}\text{O}_{\text{alg}}$  versus SST varied from  $-0.09$  to  $-0.23\text{‰}\text{°C}^{-1}$  by a factor of approximately 2.5. Positive slopes for both Arctic Bay and Maine  $\delta^{18}\text{O}_{\text{alg}}$  versus SSS varied from  $0.072\text{‰}$  to  $0.27\text{‰}\text{psu}^{-1}$  by a factor of approximately 3.75, though the Maine slope was not significant at the 95% confidence interval.

## 5. DISCUSSION

In order to constrain the  $\delta^{18}\text{O}_{\text{alg}}$ –climate relationship across the high-latitude Northern Hemisphere, we calibrated  $\delta^{18}\text{O}_{\text{alg}}$  at climatologically distinct sites, where the slope of the regression line may function as the calibrated coefficient for a PSM translating gridded SST and SSS data into  $\delta^{18}\text{O}_{\text{alg}}$ . Discrepancies in the timing, nature, and strength of the climate signal continue to require independent calibrations at each site as  $\delta^{18}\text{O}_{\text{alg}}$  is developed as a high-latitude marine climate proxy. Therefore, calibrations developed at distant locations require caution when applied locally. This is particularly an issue for SSS, as the  $\delta^{18}\text{O}_{\text{alg}}$ –SODA SSS relationship was only significant at the Arctic Bay. For SST, the slope of the  $\delta^{18}\text{O}_{\text{alg}}$ –SODA SST regression ( $-0.23\text{‰}\text{°C}^{-1}$ ) at Amchitka Island was consistent with the slope of  $-0.22\text{‰}\text{°C}^{-1}$  observed for aragonite precipitation in seawater (Grossman and Ku, 1986); however, the agreement did not hold for the Attu Island  $\delta^{18}\text{O}_{\text{alg}}$ –SST regressions (slope =  $-0.09\text{‰}\text{°C}^{-1}$  and  $-0.14\text{‰}\text{°C}^{-1}$  for NOAA ERSST and SODA SST, respectively). Nonetheless, this range of slopes for the  $\delta^{18}\text{O}_{\text{alg}}$ –SST relationship is within the range displayed by corals across individual sites ( $-0.10$  to  $-0.34\text{‰}\text{°C}^{-1}$  (Evans et al., 2000)). Furthermore, studies that synthesize coral records across a number of sites report a slope of around  $-0.22\text{‰}\text{°C}^{-1}$  (Evans et al., 2000; Lough, 2004), suggesting that additional algal records may help further constrain the  $\delta^{18}\text{O}_{\text{alg}}$ –SST relationship.

The magnitude and significance of the  $\delta^{18}\text{O}_{\text{alg}}$ –SST and  $\delta^{18}\text{O}_{\text{alg}}$ –SSS relationships must be further characterized before they may be applied universally to a PSM of encrusting algae; nonetheless, the calibrations reported here may

serve as a baseline for the development of a coralline algal PSM from which the impact of these calibration uncertainties may be further investigated. Toward this end, we discuss the factors that may contribute to variation in the  $\delta^{18}\text{O}_{\text{alg}}$ –climate relationship among sites: (1) local climatology, (2) incorporation of the climate signal into the algal skeleton, (3) interaction between SST and SSS, and (4) uncertainties in the proxy and gridded data. Physiological differences between individual organisms and between the two species may also contribute to calibration differences.

### 5.1. Local climatology

Variation in local climatology among the four sites (Fig. 2) provides an environmental explanation for differences in the magnitude and strength of calibrated coefficients. At the Aleutian sites, SST is the primary driver of  $\delta^{18}\text{O}_{\text{alg}}$  (Fig. 5) because SST varies more than SSS throughout the year and among years (Fig. 2). Aleutian SST itself is largely driven by the location of the Aleutian Low, a winter low-pressure system that brings storms to the Bering Sea (Niebauer et al., 1999; Rodionov et al., 2007). In contrast, winter sea-ice cover limits algal growth in Arctic Bay. In turn, sea-ice volume determines SSS at this site, while the seasonal ice cover and low overall SST result in small seasonal changes in SST; therefore  $\delta^{18}\text{O}_{\text{alg}}$  primarily records local SSS. In the Gulf of Maine, SST and SSS both vary considerably throughout the year and among years (Fig. 2). At this site, Halfar et al. (2008) found a significant relationship with locally recorded SST centered on the summer and fall months; however, the relationship did not hold with the gridded SST we used here, which lacked the increasing trend of the local Boothbay Harbor data set used by Halfar et al. (2008) (Fig. S4). Nonetheless, NOAA ERSST and SODA SST still significantly correlated with the Boothbay data set during eight (May–December) and four (January, October–December) months of the year, respectively (Fig. S5); annually averaged NOAA ERSST also significantly varied with annually averaged Boothbay SST ( $p = 0.032$ ,  $r = 0.43$ ,  $n = 25$ , not shown). Instead of SST, we found a relationship at the 94% confidence interval with gridded SSS in the Gulf of Maine, which may be driven by basin circulation, freshwater river input, density-driven stratification, and competing influx from warm saline Northeast Channel and cool fresh Scotian Shelf waters (Xue et al., 2000; Thompson, 2010). This SSS signal may have also contributed to the correlation between  $\delta^{18}\text{O}_{\text{alg}}$  and Boothbay SST observed by Halfar et al. (2008), as

SODA SSS significantly correlated with Boothbay SST during May ( $p = 0.036$ ,  $r = -0.42$ ,  $n = 25$ , not shown).

## 5.2. Incorporation of climate signal

Other potential environmental influences on  $\delta^{18}\text{O}_{\text{alg}}$ , such as light availability, may explain the remaining variability in  $\delta^{18}\text{O}_{\text{alg}}$  not captured by the  $\delta^{18}\text{O}_{\text{alg}}$ -SST and  $\delta^{18}\text{O}_{\text{alg}}$ -SSS relationships (Fig. S3). As with SST and SSS, the relative importance of any additional climate factors could depend on the site and the specimen; for example, larger regression residuals (and lower  $R^2$ ) of the Amchitka  $\delta^{18}\text{O}_{\text{alg}}$ -SST relationship suggests that there may be an additional physical or biological driver of  $\delta^{18}\text{O}_{\text{alg}}$  variability at this site that needs to be investigated in future work (Fig. S3).

At all sites, a lag between the source of the climate signal and detection by the algae could explain why the climate signal was sometimes detected in the winter when algae grow minimally, if at all (Fig. 5). For example, basin dynamics that influenced wintertime SSS in the Gulf of Maine could have affected summer algal growth later in the year, explaining the significant correlations between Maine  $\delta^{18}\text{O}_{\text{alg}}$  and SSS in February and March (Fig. 5).

Conversely,  $\delta^{18}\text{O}_{\text{alg}}$  could have recorded another climate parameter, e.g. light as mentioned above, during summer-fall periods of growth and calcification that was linked to subsequent changes in SST or SSS. This could explain why Amchitka  $\delta^{18}\text{O}_{\text{alg}}$  significantly correlated with SODA SST in December (Fig. 5), which fell after the expected major growth period for the year. December SSTs weakly correlated with those averaged over the March–May period (the other months when our results indicate the alga was likely growing) ( $r = 0.30$ ,  $p = 0.078$ ), suggesting that this December signal could be an artifact of the nature of the seasonal cycle at this site. If this is the case, December may not be a crucial period when the Amchitka alga recorded SST in the first place. Removing December SODA SST from the March–May average had only a minor effect on the significance and slope of the  $\delta^{18}\text{O}_{\text{alg}}$ -SST relationship (slope =  $-0.18$ ,  $R^2 = 0.16$ ,  $p = 0.016$ ; compare to slope =  $-0.23$ ,  $R^2 = 0.20$ ,  $p = 0.0063$  when December is included). In fact, removing December moved the slope of Amchitka  $\delta^{18}\text{O}_{\text{alg}}$ -SST relationship closer to that of the Attu relationship. Finally, coralline algae biology may further contribute to the winter signal; algae use stored energy to continue growing and calcifying even after low insolation in the fall prohibits photosynthesis (Adey et al., 2013). Comparing  $\delta^{18}\text{O}_{\text{alg}}$  to other proxy data derived from *Clathromorphum* sp., e.g. Mg/Ca as an established SST proxy, could help distinguish between these multiple influences on  $\delta^{18}\text{O}_{\text{alg}}$  (Kamenos et al., 2008).

## 5.3. Temperature-salinity interaction

Significant relationships between SST and SSS during some months when  $\delta^{18}\text{O}_{\text{alg}}$  recorded SST or SSS (e.g. July for Attu NOAA ERSST and SSS) suggest that  $\delta^{18}\text{O}_{\text{alg}}$  may also record an integrated SST-SSS signal (Fig. S2). However, the sparseness of these months at which SST

and SSS were significantly correlated suggests that an interaction term between SST and SSS may not ultimately be necessary for  $\delta^{18}\text{O}_{\text{alg}}$  PSMs. These high-latitude sites contrast with tropical regions where many other biomineralizers are found and SST and SSS are more strongly tied. The absence of a strong interaction between SST and SSS in high-latitude regions emphasizes the importance of including both SST and SSS in coralline algae PSMs, as these signals may confound one another.

## 5.4. Uncertainties in proxy and gridded data

Physical contributions to calibration differences are compounded by limitations and uncertainties in the proxy chronology, number of specimens, temporal coverage, and incorporation of historical observations into gridded data sets. For example, deviations between the gridded data sets and real SST and SSS could contribute to the remaining  $\delta^{18}\text{O}_{\text{alg}}$  variability unaccounted for by the calibrated  $\delta^{18}\text{O}_{\text{alg}}$ -SST and  $\delta^{18}\text{O}_{\text{alg}}$ -SSS relationships (Fig. S3). At Arctic Bay, the lower resolution of the  $\delta^{18}\text{O}_{\text{alg}}$  proxy record could have contributed to a weaker relationship with climate at this site, though the SSS relationship was robust. Minor serial correlation, which is a common feature of marine proxy records due to the red spectra of ocean climate variability, may further reduce the strength and significance of the  $\delta^{18}\text{O}_{\text{alg}}$ -climate relationship (Table 2); longer time series in future studies will increase the effective sample size and produce more robust regression results.

Historical climate observations are limited in these high-latitude regions (Figs. S6 and S7), and therefore uncertainties in the gridded datasets likely contribute to the calibration differences among sites. Such observational uncertainties are particularly large at the Arctic Bay and Maine sites, where the NOAA ERSST and SODA SST data sets are poorly correlated over the calibration interval (Fig. S1). NOAA ERSST and SODA SST also draw from different archives of observational data, with ICOADs contributing to NOAA ERSST while SODA SST uses other records including the World Ocean Database. Furthermore, these data sets use contrasting methods to incorporate observations into gridded data; NOAA ERSST uses statistical methods to fill in spatial and temporal gaps in observations, whereas SODA SST comes from an ocean circulation model forced with observations. Thus, weaknesses in the relationship between  $\delta^{18}\text{O}_{\text{alg}}$  and SODA SST or SSS may indicate weaknesses in how the ocean model simulates the physics as well as in the observation inputs. Finally, NOAA ERSST only includes the surface, whereas SODA SST includes temperatures at lower depths that better match where the algae grew. This may contribute to the weaker  $\delta^{18}\text{O}_{\text{alg}}$ -ERSST than  $\delta^{18}\text{O}_{\text{alg}}$ -SODA SST relationships at the Aleutian sites (Table 2). The combination of different observational data, different methods, different depths, and overall scarcity of high-latitude observations may account for differences in the  $\delta^{18}\text{O}_{\text{alg}}$ -SST relationship between NOAA ERSST and SODA SST (Figs. 5 and 6).

Uncertainty in the gridded data sets may also explain why the SST signal we found in Maine  $\delta^{18}\text{O}_{\text{alg}}$  was weaker than described by Halfar et al. (2008). Halfar et al. (2008)

found that declining  $\delta^{18}\text{O}_{\text{alg}}$  matched a warming trend in a local SST data set from Boothbay Harbor, whereas no notable warming is present in the gridded data sets. This suggests that either the gridded data set is too coarse to resolve local SST trends or the quality or number of observations included in the gridded data is insufficient. The second explanation is better supported for two reasons. First, the distance from the algal collection site to the Boothbay Harbor observation site is 120 km, not much less than the size of the  $2^\circ \times 2^\circ$  NOAA ERSST grid box (approximately  $150 \text{ km} \times 225 \text{ km}$ ) and notably greater than the size of the  $0.5^\circ \times 0.5^\circ$  SODA SST grid box (approximately  $37 \text{ km} \times 56 \text{ km}$ ). Second, ICOADS SST observations, which form the basis for NOAA ERSST used at Maine, were far fewer at Maine than at the Aleutian sites (Fig. S6); in fact, the average number of observations per year at Maine (79 obs/year) was only slightly greater than at Arctic Bay (62 obs/year), where several months of the year lacked observations due to sea-ice cover. While WOD observations were more abundant at Maine (Fig. S7), the number of WOD observations may not accurately represent overall observations, as satellite and other observation sources also contributed to SODA SST. Altogether, this suggests that uncertainty in the gridded data at Maine comes from limited observations.

Finally, all specimens were collected along the coast at their respective sites, whereas the gridded data sets simulated open marine conditions. Thus, the algal growth sites may have received freshwater inputs from runoff and shore-fast ice (i.e. sea ice attached to the coastline), which were not included in the gridded data sets. Furthermore, SST and circulation models used to construct SODA SST and SSS may not have adequately represented coastal dynamics influencing algal growth, e.g. coastal upwelling and shelf-slope exchange along the Aleutian archipelago (Stabeno et al., 1999). NOAA ERSST would not have been affected by model representation of coastal dynamics, as it uses observations and statistical models rather than a circulation model.

Nevertheless, the calibration with gridded rather than local data is useful for assessing the feasibility of using gridded data throughout the algal habitat range and for comparing coralline algae calibrations among sites. Gridded data are the only marine climate data available at some coralline algae sites, as they are available globally while in situ data are limited in coverage; therefore this analysis provides an essential step toward assessing the limitations of these data sets in regions where coralline algae may be used as marine climate archives.

## 6. SUMMARY AND IMPLICATIONS

We calibrated  $\delta^{18}\text{O}_{\text{alg}}$  to gridded SST and SSS at four diverse sites to advance our understanding of the  $\delta^{18}\text{O}_{\text{alg}}$ –climate relationship and to assess whether the slopes of the  $\delta^{18}\text{O}_{\text{alg}}$ –climate relationship converge across the algal habitat range. Significant relationships with SST at Amchitka and Attu Islands and to SSS at Arctic Bay supported  $\delta^{18}\text{O}_{\text{alg}}$  as marine climate proxy at crucial high latitudes; however, variation in the timing, nature, and

strength of the climate signal indicated that site-specific calibrations are necessary for algal climate reconstructions or PSMs. In addition, we found preliminary evidence for a coupled SST–SSS signal requiring further investigation.

In evaluating the globally gridded data sets used in this study, we identified limitations in gridded data that should be considered as these data continue to be applied to calibrate proxy–climate relationships of coralline algae and other climate proxy systems, particularly at high latitudes. Comparisons among gridded data sets and between gridded data and in situ observations at more sites would be useful to characterize the discrepancies between interpolated or simulated climate records and actual climate conditions throughout the global oceans.

As gridded data continue to be improved, calibrating additional specimens over longer time periods could help reduce uncertainty from the biological system. Multiple specimens at each site would help filter out organism specificity and other non-climatic factors (Lough, 2004). Averaging multiple specimens has been shown to strengthen the Mg/Ca–SST signal and is likely to do the same for  $\delta^{18}\text{O}_{\text{alg}}$  (Williams et al., 2014). The short time period ranging from 25 to 42 years restricts us from employing more robust calibration methods, such as separating the analysis into calibration and verification sub-periods (Williams et al., 2014), and grants little opportunity to capture multi-year fluctuations to which algae may be more sensitive than year-to-year changes (Halfar et al., 2007). In future work we will also further investigate the role of uncertainty in SST and SSS observations in the calibration estimates using reduced major axis and weighted least squares regression approaches with SST and SSS data sets for which error estimates are available (York et al., 2004; Thirumalai et al., 2011).

Despite the low sample size and short time period, we show here a reasonably constrained SST relationship; the slope of significant Aleutian calibrations fell within a factor of 2.5, well within the range of slopes observed across corals from different sites (Evans et al., 2000; Lough, 2004). We have also shown a significant SSS relationship, which has not previously been established, at the Arctic Bay site. However, the SSS relationship was poorly constrained, as the slope of the relationship varied by a factor of 3.5 between the Arctic Bay and (non-significant) Maine calibrations. This is unsurprising considering that the seawater  $\delta^{18}\text{O}$ –SSS relationship depends on site-specific water sources and that the climatic environment differs greatly among the Aleutian Islands, Arctic Bay, and the Gulf of Maine. Additional long-term records may further constrain the  $\delta^{18}\text{O}_{\text{alg}}$ –climate relationship across the algal habitat range.

This work takes an essential intermediate step toward reconstructing regional climate patterns with coralline algae. Previous studies have moved from describing physiology and ecology to reconstructing SST at single sites; we have now moved from single sites to multiple sites spanning much of the algal habitat. With further calibration refinements,  $\delta^{18}\text{O}_{\text{alg}}$  may enhance our understanding of basin-scale oscillations, links between Pacific and Atlantic oscillations, and impending changes in vulnerable Arctic seas.

## ACKNOWLEDGEMENTS

We are grateful to our reviewers for suggesting substantial improvements to the statistical methods and structure of the paper. Funding was provided by NSF Award 1459827 to BW which supported JN, the Advanced Study Program at the National Center for Atmospheric Research to DT, NSERC Discovery Grant #316003 to JH, and ArcticNet NCE Grant to EE.

## APPENDIX A. SUPPLEMENTARY DATA

Supplementary data associated with this article can be found, in the online version, at <http://dx.doi.org/10.1016/j.gca.2016.08.023>.

## REFERENCES

- Adey W. H. (1965) The genus *Clathromorphum* (Corallinaceae) in the Gulf of Maine. *Hydrobiologia* **26**, 539–573. <http://dx.doi.org/10.1007/BF00045545>.
- Adey W. H., Halfar J. and Williams B. (2013) The coralline genus *Clathromorphum* Foslie emend. Adey: Biological, physiological, and ecological factors controlling carbonate production in an arctic-subarctic climate archive. *Smithsonian Contrib. Mar. Sci.* **40**, 41.
- Biondi F. and Waikul K. (2004) DENDROCLIM2002: A C++ program for statistical calibration of climate signals in tree-ring chronologies. *Comput. Geosci.* **30**, 303–311. <http://dx.doi.org/10.1016/j.cageo.2003.11.004>.
- Brohan P., Kennedy J. J., Harris I., Tett S. F. B. and Jones P. D. (2006) Uncertainty estimates in regional and global observed temperature changes: a new data set from 1850. *J. Geophys. Res.* **111**, D12106. <http://dx.doi.org/10.1029/2005JD006548>.
- Butler P., Wanamaker A., Scourse J. D., Richardson C. A. and Reynolds D. J. (2013) Variability of marine climate on the North Icelandic Shelf in a 1357-year proxy archive based on growth increments in the bivalve *Arctica islandica*. *Palaeogeogr. Palaeoclimatol. Palaeoecol.* **373**, 141–151. <http://dx.doi.org/10.1016/j.palaeo.2012.01.016>.
- Carton J. A. and Giese B. S. (2008) A reanalysis of ocean climate using Simple Ocean Data Assimilation (SODA). *Mon. Weather Rev.* **136**, 2999–3017. <http://dx.doi.org/10.1175/2007MWR1978.1>.
- Correge T. (2006) Sea surface temperature and salinity reconstruction from coral geochemical tracers. *Palaeo3* **232**, 408–428. <http://dx.doi.org/10.1016/j.palaeo.2005.10.014>.
- Cullen L. and Grierson P. F. (2009) Multi-decadal scale variability in autumn-winter rainfall in south-western Australia since AD 1655 as reconstructed from tree rings of *Callitris columellaris*. *Clim. Dyn.* **33**, 433–444. <http://dx.doi.org/10.1007/s00382-008-0457-8>.
- Curry J. A., Schramm J. L. and Ebert E. E. (1995) Sea ice-albedo climate feedback mechanism. *J. Clim.* **8**, 240–247. [http://dx.doi.org/10.1175/1520-0442\(1995\)008<0240:SIACFM>2.0.CO;2](http://dx.doi.org/10.1175/1520-0442(1995)008<0240:SIACFM>2.0.CO;2).
- de Vernal A., Rosell-Mele A., Kucera M., Hillaire-Marcel C., Eynaud F., Weinelt M., Dokken T. and Kageyama M. (2006) Comparing proxies for the reconstruction of LGM sea-surface conditions in the northern North Atlantic. *Quat. Sci. Rev.* **25**, 2820–2834. <http://dx.doi.org/10.1016/j.quascirev.2006.06.006>.
- Dee S. G., Steiger N. J., Emile-Geay J. and Hakim G. J. (2016) On the utility of proxy system models for estimating climate states over the common era. *J. Adv. Model. Earth Syst.* <http://dx.doi.org/10.1002/2016MS000677>. Accepted author manuscript.
- Epstein S., Buchsbaum R., Lowenstam H. and Urey H. C. (1951) Carbonate-water isotopic temperature scale. *Bull. Geol. Soc. Am.* **62**, 417–426. <http://dx.doi.org/10.1130/0016-7606>.
- Evans M. N., Kaplan A. and Cane M. A. (2000) Intercomparison of coral oxygen isotope data and historical sea surface temperature (SST): potential for coral-based SST field reconstructions. *Paleoceanography* **15**, 551–563. <http://dx.doi.org/10.1029/2000PA000498>.
- Evans M. N., Tolwinski-Ward S. E., Thompson D. M. and Anchikaitis K. J. (2013) Applications of proxy system modeling in high resolution paleoclimatology. *Quat. Sci. Rev.* **76**, 16–28. <http://dx.doi.org/10.1016/j.quascirev.2013.05.024>.
- Fritts H. C. (1976) *Tree Rings and Climate*. Academic Press, London.
- Grossman E. L. and Ku T. L. (1986) Oxygen and carbon isotopic fractionation in biogenic aragonite: temperature effects. *Chem. Geol. (Isot. Geosci. Sect.)* **59**, 59–74. [http://dx.doi.org/10.1016/0168-9622\(86\)90057-6](http://dx.doi.org/10.1016/0168-9622(86)90057-6).
- Halfar J., Steneck R., Schöne B., Moore G. W. K., Joachimski M., Kronz A., Fietzke J. and Estes J. (2007) Coralline algae reveals first marine record of subarctic North Pacific climate change. *Geophys. Res. Lett.* **34**, L07702. <http://dx.doi.org/10.1029/2006GL028811>.
- Halfar J., Steneck R. S., Joachimski M., Kronz A. and Wanamaker A. D. (2008) Coralline red algae as high-resolution climate recorders. *Geology* **36**, 463–466. <http://dx.doi.org/10.1130/G24635A.1>.
- Halfar J., Adey W. H., Kronz A., Hetzinger S., Edinger E. and Fitzhugh W. W. (2013) Arctic sea-ice decline archived by multicentury annual-resolution record from crustose coralline algal proxy. *Proc. Natl. Acad. Sci. USA* **110**, 19737–19741. <http://dx.doi.org/10.1073/pnas.1313775110>.
- Halfar J. et al. (2011) 225 years of Bering Sea climate and ecosystem dynamics revealed by coralline algal growth-increment widths. *Geol. Soc. Am. Data Rep. Geol.*
- Hegerl G. C., Crowley T. J., Hyde W. T. and Frame D. J. (2006) Climate sensitivity constrained by temperature reconstructions over the past seven centuries. *Nature* **440**, 1029–1032. <http://dx.doi.org/10.1038/nature04679>.
- Hetzinger S., Halfar J., Kronz A., Steneck R. S., Adey W., Lebednik P. A. and Schöne B. R. (2009) High-resolution Mg/Ca ratios in a coralline red alga as a proxy for Bering Sea temperature variations from 1902 to 1967. *Palaios* **24**, 406–412. <http://dx.doi.org/10.2110/palo.2008.p08-116r>.
- Hetzinger S., Halfar J., Meckling J. V., Keenlyside N. S., Kronz A., Steneck R. S., Adey W. H. and Lebednik P. A. (2012) Marine proxy evidence linking decadal North Pacific and Atlantic climate. *Clim. Dyn.* **39**, 1447–1455. <http://dx.doi.org/10.1007/s00382-011-1229-4>.
- Huang B., Banzon V. F., Freeman E., Lawrimore J., Liu W., Peterson T. C., Smith T. M., Thorne P. W., Woodruff S. D. and Zhang H. (2015) Extended reconstructed sea surface temperature version 4 (ERSST.v4). Part I: upgrades and intercomparisons. *J. Clim.* **28**, 911–930. <http://dx.doi.org/10.1175/JCLI-D-14-00006.1>.
- Huang J., Tardif J. C., Bergeron Y., Denneler B., Berninger F. and Girardin M. P. (2010) Radial growth response of four dominant boreal tree species to climate along a latitudinal gradient in the eastern Canadian boreal forest. *Glob. Change Biol.* **16**, 711–731. <http://dx.doi.org/10.1111/j.1365-2486.2009.01990.x>.
- Kamenos N. A., Cusack M. and Moore P. G. (2008) Coralline algae are global paleothermometers with bi-weekly resolution. *Geochim. Cosmochim. Acta* **72**, 771–779. <http://dx.doi.org/10.1016/j.gca.2007.11.019>.
- Kamenos N. A., Hoey T. B., Nienow P., Fallick A. E. and Claverie T. (2012) Reconstructing greenland ice sheet runoff using

- coralline algae. *Geology* **40**, 1095–1098. <http://dx.doi.org/10.1130/G33405.1>.
- Kirtman B., Power S. B., Adedoyin J. A., Boer G. J., Bojariu R., Camilloni I., Doblas-Reyes F. J., Fiore A. M., Kimoto M., Meehl G. A., Prather M., Sarr A., Schär C., Sutton R., van Oldenborgh G. J., Vecchi G. and Wang H. J. (2013) Near-term climate change: projections and predictability. In *Climate Change 2013: The Physical Science Basis. Contribution of Working Group I to the Fifth Assessment Report of the Intergovernmental Panel on Climate Change* (eds. T. F. Stocker, D. Qin, G.-K. Plattner, M. Tignor, S. K. Allen, J. Boschung, A. Nauels, Y. Xia, V. Bex and P. M. Midgley). Cambridge University Press, Cambridge, United Kingdom and New York, NY, USA.
- Lebednik P. (1976) The Corallinaceae of Northwestern North America. I. *Clathromorphum* Foslie emend. Adey. *Syesis* **9**, 59–112.
- Lee D. E. and Carpenter S. J. (2001) Isotopic dis-equilibrium in marine calcareous algae. *Chem. Geol.* **172**, 307–329. [http://dx.doi.org/10.1016/S0009-2541\(00\)00258-8](http://dx.doi.org/10.1016/S0009-2541(00)00258-8).
- LeGrande A. N. and Schmidt G. A. (2006) Global gridded data set of the oxygen isotopic composition in seawater. *Geophys. Res. Lett.* **33**, L12604. <http://dx.doi.org/10.1029/2006GL026011>.
- Liang E., Dawadi B., Pederson N. and Eckstein D. (2014) Is the growth of birch at the upper timberline in the Himalayas limited by moisture or by temperature? *Ecology* **95**, 2453–2465. <http://dx.doi.org/10.1890/13-1904.1>.
- Liu W., Huang B., Thorne P. W., Banzon V. F., Zhang H., Freeman E., Lawrimore J., Peterson T. C., Smith T. M. and Woodruff S. D. (2015) Extended reconstructed sea surface temperature version 4 (ERSST.v4): Part II. Parametric and structural uncertainty estimations. *J. Clim.* **28**, 931–951. <http://dx.doi.org/10.1175/JCLI-D-14-00007.1>.
- Lough J. M. (2004) A strategy to improve the contribution of coral data to high-resolution paleoclimatology. *Palaeogeogr. Palaeoclimatol. Palaeoecol.* **204**, 115–143. [http://dx.doi.org/10.1016/S0031-0182\(03\)00727-2](http://dx.doi.org/10.1016/S0031-0182(03)00727-2).
- Meehl G. A., Washington W. M., Arblaster J. M., Hu A., Teng H., Tebaldi C., Sanderson B. N., Lamarque J.-F., Conley A., Strand W. G. and White J. B. I. I. I. (2012) Climate system response to external forcings and climate change projections in CCSM4. *J. Clim.* **25**, 3661–3683. <http://dx.doi.org/10.1175/JCLI-D-11-00240.1>.
- Meehl G. A., Washington W. M., Arblaster J. M., Hu A., Teng H., Kay J. E., Gettelman A., Lawrence D. M., Sanderson B. M. and Strand W. G. (2013) Climate change projections in CESM1 (CAM5) compared to CCSM4. *J. Clim.* **26**, 6287–6308. <http://dx.doi.org/10.1175/JCLI-D-12-00572.1>.
- Moberly R. (1968) Composition of magnesian calcites of algae and pelecypods by electron microprobe analysis. *Sedimentology* **11**, 61–82. <http://dx.doi.org/10.1029/2006GL028811>.
- Niebauer H. J., Bond N. A., Yakunin L. P. and Plotnikov V. V. (1999) An update on the climatology and sea ice of the bering sea. In *Dynamics of the Bering Sea: A Summary of Physical, Chemical, and Biological Characteristics, and a Synopsis of Research on the Bering Sea* (eds. T. R. Loughlin and K. Ohtani). North Pacific Marine Science Organization (PICES), University of Alaska Sea Grant, AK-SG-99-03, pp. 1–28.
- PAGES 2k Consortium (2013) Continental-scale temperature variability during the past two millennia. *Nat. Geosci.* **6**, 339–346. <http://dx.doi.org/10.1038/ngeo1797>.
- Rodionov S. N., Bond N. A. and Overland J. E. (2007) The Aleutian Low, storm tracks, and winter climate variability in the Bering Sea. *Deep-Sea Res. II* **54**, 2560–2577. <http://dx.doi.org/10.1016/j.dsr2.2007.08.002>.
- Schmidt G. A. (1999) Forward modeling of carbonate proxy data from planktonic foraminifera using oxygen isotope tracers in a global ocean model. *Paleoceanography* **14**, 482–492. <http://dx.doi.org/10.1029/1999PA900025>.
- Surge D. and Barrett J. H. (2012) Marine climatic seasonality during medieval times (10th to 12th centuries) based on isotopic records in Viking Age shells from Orkney, Scotland. *Palaeogeogr. Palaeoclimatol. Palaeoecol.* **350–352**, 236–246. <http://dx.doi.org/10.1016/j.palaeo.2012.07.003>.
- Stabeno P., Schumacher J. D. and Ohtani K. (1999) The physical oceanography of the bering sea. In *Dynamics of the Bering Sea: A Summary of Physical, Chemical, and Biological Characteristics, and a Synopsis of Research on the Bering Sea* (eds. T. R. Loughlin and K. Ohtani). North Pacific Marine Science Organization (PICES), University of Alaska Sea Grant, AK-SG-99-03, pp. 1–28.
- Thirumalai K., Singh A. and Ramesh R. (2011) A MATLAB™ code to perform weighted linear regression with (correlated or uncorrelated) errors in bivariate data. *J. Geol. Soc. India* **77** (April), 377–380. <http://dx.doi.org/10.1007/s12594-011-0044-1>.
- Thompson C. (2010) *The Gulf of Maine in context: State of the Gulf of Maine Report*. Gulf of Maine Council on the Marine Environment.
- Thompson D. M., Ault T. R., Evans M. N., Cole J. E. and Emile-Geay J. (2011) Comparison of observed and simulated tropical climate trends using a forward model of coral  $\delta^{18}\text{O}$ . *Geophys. Res. Lett.* **38**, L14706. <http://dx.doi.org/10.1029/2011GL048224>.
- Wanamaker A. D., Butler P. G., Scourse J. D., Heinemeier J., Eiríksson J., Knudsen K. L. and Richardson C. A. (2012) Surface changes in the North Atlantic meridional overturning circulation during the last millennium. *Nat. Commun.* **3**, 899. <http://dx.doi.org/10.1038/ncomms2901>.
- Williams B., Halfar J., DeLong K. L., Hetzinger S., Steneck R. S. and Jacob D. E. (2014) Multi-specimen and multi-site calibration of Aleutian coralline algal Mg/Ca to sea surface temperature. *Geochim. Cosmochim. Acta* **139**, 190–204. <http://dx.doi.org/10.1016/j.gca.2014.04.006>.
- Williams B., Halfar J., Steneck R. S., Wortmann U. G., Hetzinger S., Adey W., Lebednik P. and Joachimski M. (2011) Twentieth century  $\delta^{13}\text{C}$  variability in surface water dissolved inorganic carbon recorded by coralline algae in the northern North Pacific Ocean and the Bering Sea. *Biogeosciences* **8**, 165–174. <http://dx.doi.org/10.5194/bg-8-165-2011>.
- Xue H., Chai F. and Pettigrew N. R. (2000) A model study of the seasonal circulation in the Gulf of Maine. *J. Phys. Oceanogr.* **30**, 1111–1135. <http://dx.doi.org/10.1175/1520-0485>.
- York D., Evensen N. M., Martínez M. L. and Delgado J. D. B. (2004) Unified equations for the slope, intercept, and standard errors of the best straight line. *Am. J. Phys.* **72**, 367. <http://dx.doi.org/10.1119/1.1632486>.

Associate editor: Jack Middelburg